*EVS27*
*Barcelona, Spain, November 17-20, 2013*

# Analytical thermal model for characterizing a Li-ion battery cell

Cicconi P., Germani M. , Landi D.[1]
[1] *Università Politecnica delle Marche, via Brecce Bianche, 60131 – Ancona – Italy, d.landi@univpm.it*

## Abstract

In a scenario of small and customized production of electric vehicle, it is important to set methods and tools to evaluate the Li-Ion cells heat source in EV battery. The main problem of the new lithium batteries is represented by the need to keep the battery packs at uniform and constant temperatures and avoid peaks of temperatures which cause degradation of performance and safety problem. The main issue concerns the characterization of a thermal model to calculate the heat generated by electrochemical reactions in a single battery cell. In order to achieve this objective, electrical tests have been conducted to obtain the parameters such as voltage curves, open circuit voltage, and capacity for different type of Li-Ion cells and different rate of current in charge and discharge. During experiments, the use of an IR camera allows to acquire real temperature data under working conditions. These tests concern one cell per time, analyzed in natural convection condition at constant external temperature. The heat generation is evaluated solving the analytical thermal formula which depends on the current rate. The approach has been validated comparing the calculated temperature values with experimental data. The proposed methodology allows to determine the heat generated and temperature for different working condition.

*Keywords: lithium battery, heat exchange, modeling*

## 1 Introduction

An important target of European environmental policy is to improve air quality both in large cities and small city-centers by reducing smog and pollution which is mainly caused by exhaust gases and particulates emitted from vehicles internal combustion engines. Many research activities concern the improvement of electric powertrain solution for EVs (Electric Vehicles) and HEVs (Hybrid Electric Vehicles). The attention is mainly focused on high efficiency electric motors, energy management, energy supply and battery efficiency. In particular, battery development is essential to replace fossil fuel on high efficiency pure-electric vehicles or in hybrid-electric ones. Electric powertrain requirements are: energy availability, high storage capacity battery and long lasting high power, high system efficiency, safety and little weight to improve vehicle performances.

Most battery applications for HEVs and EVs use lithium-ion battery packs composed of several cells. In particular the $LiFePO_4$ (lithium iron phosphate, also called LFP) polymeric cells provide high voltage, low self-discharge rate [1][2] and high energy density suitable for a wide range of applications. The main drawbacks are: high manufacturing cost, long-term stability and poor safety characteristics caused by high heat generation produced by electrochemical reactions during charge/discharge cycles [3]. In electric vehicles, battery temperature increases with a high charge and discharge rate, especially in transitory utilization. Excessive temperature degrades performance, and a limited thermal dissipation can produce cell burning [4]. Several recent studies have analyzed two aspect for lithium-ion batteries: the perspective of a deep electrochemical characterization through study of ion concentrations and electrons moving to evaluate voltage and state of charge at different current rate, and the thermal behavior analysis with numerical simulations and experimental tests to optimize the cooling system. The proposed research presents a working methodology which allows to determine the heat generated from a single cell at different working conditions. All this allows to obtain the cell average temperature, and to support the designer in the definition of suitable cooling system. The present work focuses the design of custom battery packs for automotive, but can be applied to any use of the batteries, such as UPS.

# 2 Background research

The performance, life, and safety of lithium-ion batteries depend on operative and storage temperatures. In this section a brief overview of main theories studied for the determination of the heat generated by electrochemical reactions in lithium-ion batteries. The batteries heat generation is a complex process that requires the comprehension of the electrochemical reaction rates change with time and temperature and of current distribution within larger batteries. Many researchers have studied thermal heat dissipation characteristics both inside one cell and inside a battery pack. The heat output in lithium-ion batteries is generated by three sources: activation (on kinetics interfacial), concentration (transport species), and ohmic losses (also known as Joule heating due to particles moving in electric circuit). A first important study, regarding electrochemical and thermal analysis of lithium-ion batteries, was made by Bernardi [5]. In this analysis, the heat generated depends on the thermodynamic equilibrium inside each cell. The first law of thermodynamics is applied around the control volume (excluding connectors), as reported in Eq. (1) formulated by Bernardi [5].

$$\dot{Q} = I(V - E_0) - IT\frac{\partial E_0}{\partial T} - \sum_i \Delta H_i^{avg} r_i - \int \sum_j \left(\overline{H}_j - \overline{H}_j^{avg}\right)\frac{\partial c_j}{\partial t}\,dv \qquad (1)$$

Then, Rao and Newman [6] observed the calculation of heat generated would have been analyzed by two different approaches: the thermodynamic energy balance, and the method of local heat generation. For the energy balance, they neglected some phase changes and the mixing effects. However they used the average local concentration in each phase to determine the rate of enthalpy change for each species and phases inside the battery. They have neglected the concentration dependence of the reference enthalpy. Applying Faraday's law, Rao and Newman arrived at the following expression for the battery heat generation in Eq. (2).

$$q = -\int_v \left(\sum_l \; a i_{n,l} U_{h,l} dv\right) - IV \qquad (2)$$

The integral term in Eq. (2) is the average enthalpy potential where the reactions are actually taking place across the thickness of the battery. For this method, Rao and Newman neglect phase changes, concentration gradients in the electrolyte phase, and thermal effects from lithium diffusion. In this approach the temperature of the cell is assumed to be uniform.

Afterwards, Thomas and Newman studied the heat due to mixing effect inside a battery containing a porous insertion electrode. They noted that, although Rao and Newman neglected mixing effects, they really did account for the heat of mixing inside the bulk electrode through variation in local current density on the effective electrode open circuit potential [7]. This is one of the four possible mixing inside the cell. The other modes of mixing heat regarding concentration gradients inside the spherical particles, bulk electrolyte, and inside the electrolyte pores of the insertion electrode. In order to calculate the enthalpy of mixing in each case, Thomas and Newman determined expressions for the difference in enthalpy from the operating state to the relaxed state using a Taylor-series expansion for the molar enthalpy of each species, while neglecting density and temperature changes and concentration dependence on the second derivative of partial molar volume with respect to partial molar enthalpy. Although these mathematical formulations are very accurate, they require many information regarding materials and each sub-layer for Li-ion cells.

Usually the designer of lithium-ion battery packs needs of a methodology based on the elaboration of few available data, due to difficult to solve completely the previous described equations. A

solution is the application of the simplified Eq. (5) analyzed by Thomas and Newman [7].
Furthermore, the scenario considered involves the use of rapid design methods for small and medium-sized enterprises, which produce and sale customized products and need to reduce the lead time to market.
In the following paragraphs the simplified formula of Bernardi will be analyzed and applied to different type of cells.

# 3 Thermal Characterization

The thermal characterization of a lithium-ion battery is an important step to evaluate the performance, lifetime and safety of a battery. In particular, the research work focuses the thermal characterization of cell model. The behavior of temperature distribution is an important aspect that every designer have to take into account in the definition and design of lithium-ion storage systems.

## 3.1 Analytical approach

The study of Bernardi [5] is considered the milestone of all subsequent research on electrochemistry regarding lithium-ion batteries. Analyzing Eq. (1), that indicates the thermal load due to the electrochemical reactions, term $\dot{Q}$ indicates the heat generated, $V$ the cell voltage, $E_0$ the OCV (open circuit voltage), $I$ the current ($I$ is >0 in charge phase and <0 in discharge one), $T$ the temperature, $\Delta H_i^{avg}$ the variation of enthalpy of a chemical reaction i, $r_i$ the rate of reaction i, $\overline{H}_j^{avg}$ the partial molar enthalpy of species j, $c_j$ its concentration, with t the time, υ the volume and the apex “avg” indicates a property evaluated at the averaged volume concentration [8].
The proposed thermal approach is based on a study by Thomas and Newman [7] which evaluates the heat produced by single cell. In particular Eq. (1) can be simplified in the first two terms: one is the exothermic and irreversible heat and the other one is the heat due to entropy changes of specifics reactions. This latter can be either endothermic or exothermic in function of current and state of charge.
The term $I(V-E_0)$ is the irreversible heat generated by Joule effect, its value is always positive (exothermic reaction) and depends on the internal resistance $R_i$, as reported in Eq. (3).

$$\dot{Q}_{irr} = I(V-E_0) = I^2 R_i \qquad (3)$$

The expression $IT\partial E_0/\partial T$ indicates the reversible heat generated by the entropy change and reported in Eq. (4). Specifying, the ratio $\partial E_0/\partial T$ can be replaced as ΔS/nF , when ΔS is the entropy change of the cell reaction which can be either positive or negative (reduction reaction), n indicates the number of exchanged electrons and F is the Faraday’s constant.

$$\dot{Q}_r = IT\frac{\partial E_0}{\partial T} = T\Delta S\frac{I}{nF} \qquad (4)$$

The last two terms in Eq. (1) can be neglected [10]; one depends on side reactions accounting for aging which are assumed to be slow enough to be neglected, and the other one is the heat of mixing which is due to the formation and relaxation of concentration gradients within the cell. This term can be considered almost zero because materials used have good electrochemical transport properties so concentration gradients are limited and the heat of mixing can be ignored. Considering the geometry of a small pouch cell and the materials, we can consider negligible the last two terms and consider the relationship of heat generation as follows.

$$\dot{Q} = Q_{irr+}Q_r = I(V-E_0) - IT\frac{\partial E_0}{\partial T} \qquad (5)$$

Temperature is the major impact factor on battery behavior and it influences all occurring processes such as chemical and electrochemical reactions, mass transport and conductivity of electrodes and electrolyte.

## 3.2 Calculation methodology

The aim of proposed analysis is the evaluation of the average temperature for a single cell during operative phase. The cooling fluid, considered in this research, is air, but the same procedure can be extended to other Newtonian fluid. Thus, Eq. (6) proposes the main energy balance between the generated electrochemical reaction heat, the convective cooling and the variation of thermal capacity. Specifically, term $h_{comb}$ is the heat transfer coefficient which includes convective and radiation aspects, term A is the external surface of one cell, term $m_{cell}$ and $c_p$ regard mass and specific heat capacity, term $T_\infty$ indicates the fluid temperature (cooling temperature); term T is the average internal temperature of cell and $T_{sup}$ is the superficial temperature [9]. The analyzed cells are slim, that means that the thickness value is very small than width and height. Due to this, our approach considers the same average value for both internal and external temperature. So, the superficial temperature is approximated to the internal value in order to consider the particular thin geometry of pouch cells.

$$I(V - E_0) + IT\frac{\partial E_0}{\partial T} = h_{comb}\left(T_{sup} - T_\infty\right)A + m_{cell}c_{p_{cell}}\frac{dT}{dt} \tag{6}$$

Temperature variation (expressed by dT/dt) is the difference between the final and the initial value of temperature during a short period of time.
The solution process has been implemented at geometry domain of a single cell, so temperature, heat capacity and voltage are expressed at average condition. Figure 1 shows the thermal balance of one cell. The proposed approach can be also extended to whole battery pack, however the complexity of cooling flow requires a CFD analysis for a 3D model of battery pack.

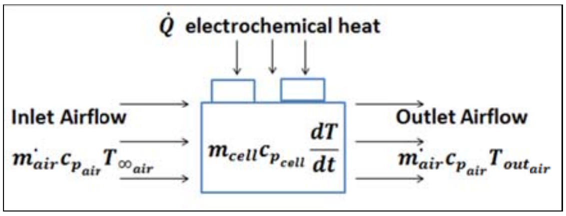


Figure 1 Thermal balance for one cell

It has been also considered the Equation (7) to solve the cooling issue, in particular the balance between the heat exchanged between air flow and cell.

$$\dot{m_{air}}c_{p_{air}}\left(T_{out_{air}} - T_{\infty_{air}}\right) = \\ = h_{comb}\left(T_{sup} - T_\infty\right)A \tag{7}$$

The first term of equation concerns the air mass flow and the difference between outlet flow temperature ($T_{out_{air}}$) and the input value ($T_{\infty_{air}}$). Matching Eq. (1) and Eq. (2) it is possible to solve the balance between the electrochemical heat and the thermal dissipation.
The thermal model allows the designer to determine how much heat is generated by one cell for different current profiles in every operative condition. In the following section the explanation about the setup of electrical test is useful for the characterization of model parameters.

### 3.3 Electrical Analysis

The electrical analysis allows to measure parameters such as: current, voltage, OCV (open circuit voltage). These parameters are useful to determine the heat generated and to solve Eq. (5).
A defined protocol has been defined to measure the electrical values. Each test reproduces cycles of charge and discharge. The main parameter is the current rate, which characterizes the electrical behavior and the resultant output voltage on battery connectors.
The OCV behavior at several values of SOC and its variation at average temperature ($\partial E_0/\partial T$) have been mapped through experimental tests on several cells used during the research activity.
Figure 2 describes the flow of experimental test and the electrical quantities analyzed for the thermal characterization of one Li-Ion cell. The battery element (cell) is maintained at a constant temperature in a climatic chamber, where it is connected to a cycler device.
The cycler is a device which can continually charge and discharge the battery, keeping a specific current profile during the test. In particular, the cycler transforms the network alternating current into the direct current which is required for the Li-ion battery to work.
An host PC is linked to cycler, in order to acquire and record experimental data in real time. Thus it is possible to monitor current rate, voltage profile, SOC and the internal resistance.
The main tests are: charge and discharge at constant current rate, and OCV measurements to achieve the physical parameters useful for the cell thermal characterization.

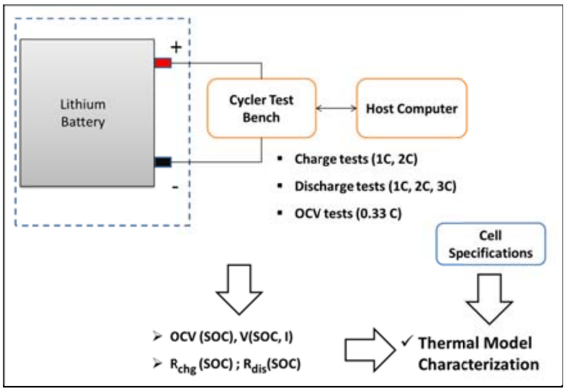


Figure 2 Flow of electrical test and physical quantities analyzed

## 4 Analytical result

The proposed approach wants to validate the analytical model in Eq. (6) for different type of Li-Ion cell. Particularly, different soft-pouch cells have been analyzed of 14Ah, 20Ah and 150Ah in capacity. This approach focused on the thermal behavior of a single soft pouch cell at several current conditions. Some experiments have been conducted at the test bench in order to achieve the necessary data for the thermal characterization of a cell. An IR (Infra-Red) camera has been used to monitor the real temperature distribution during experiment tests.

## 4.1 Test definition

Experimental tests have been conducted to achieve the profile of variation regarding the voltage and OCV state in function of SOC (state of charge). The voltage curves, related to specific current rate, have been acquired from cycler test and then elaborated in an application tool, developed to solve the analytical formula and to calculate the heat output and temperature profile depending on time and current rate. During each test, the real temperature distribution has been monitored by an IR camera. The selected cells are mostly used in automotive and UPS (uninterruptible power supply) application, due to the high power-density related to its weight.

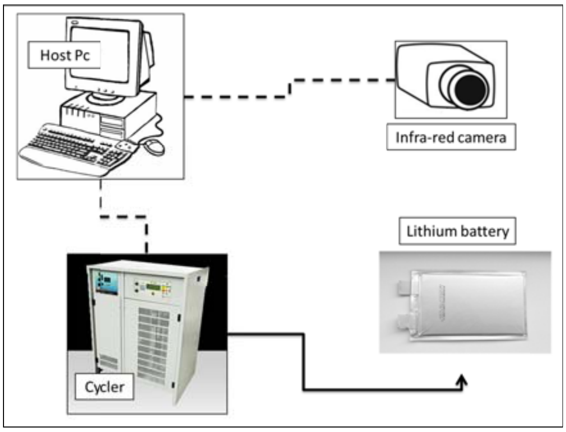


Figure 3 The test bench

Figure 3 shows a basic representation of the laboratory test layout, used for the acquisition of experimental data. The main components are: the cycler, the host PC, the IR camera and the Li-Ion cell.

The instrumentation allows to acquire the main electrical quantities such as: voltage (V), current (A), energy (W), capacity (Ah) power (W), SOC (%), and internal resistance (ohm).

As before mentioned, an host PC enables all the parameters to be monitored in real time and recorded (i.e. 1 sec. frequency). This component makes an interaction bridge between the cycler and the IR camera, where the IR camera measures the battery thermal profile. Then, an advanced software allows the temperature values to be elaborated and reported in tables and graphs.

Table 1 shows the main characteristics of the three cells analyzed (14 Ah, 20Ah and 150 Ah), which have the same geometrical aspect but different characteristics.

Table 1 Battery Li-ion cells data sheet

| Type | | 1 | 2 | 3 |
|---|---|---|---|---|
| Chemical | | $LiFePO_4$ | $LiNiCoMnO_2$ | $LiFePO_4$ |
| Geometry | | Soft Pouch | Soft Pouch | Soft Pouch |
| Dim | Length | 222 mm | 216 mm | 327 mm |
| | Width | 129 mm | 129 mm | 453 mm |
| | Thick | 7.2 | 7.2 | 10.7 |
| Nom. Voltage | | 3.25 V | 3.65V | 3.7 V |
| Nom. Capacity | | 14 Ah | 20 Ah | 150Ah |
| Max Discharge | | 140 A | 100 A | 300 A |
| Max charge | | 14 A | 20 A | 150 A |
| Weight | | 380 g | 425 g | 3300 g |

## 4.2 Electrical test result

In order to validate the proposed methodology, the cells in Table 1 have been tested at several current rates in charge and discharge mode. The figures below (Figure 4 - Figure 9) show the voltage profiles during charge and discharge for each cell analyzed. The graphs are related to SOC (state of charge) for the charge phase, while for discharge phase the values are related to DOD (depth of discharge). Each cell have been tested for different current values in charge and discharge, according to the technical datasheets (Table 1).

Each test has been carried out in a climatic chamber at a constant temperature of 25°C, under the heat transfer condition of natural convection. As result, the graphs below show reports regarding the voltage profile for each battery element.

Figure 4 represents the trend of voltage curve during charge at 1C for cell type 1 (14 Ah, $LiFePO_4$).

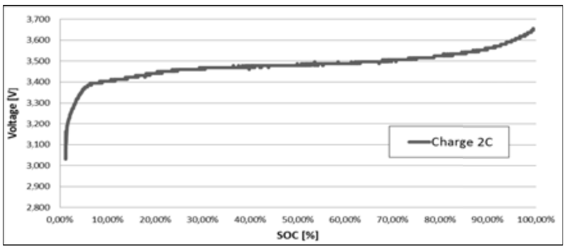


Figure 4 Voltage curve at 1C in charge for soft-pouch cell of 14Ah (type 1; chemistry: $LiFePO_4$)

Figure 5 represents the trend of voltage curves during discharge at 1C, 5C and 10C for cell type 1 (14 Ah, $LiFePO_4$).

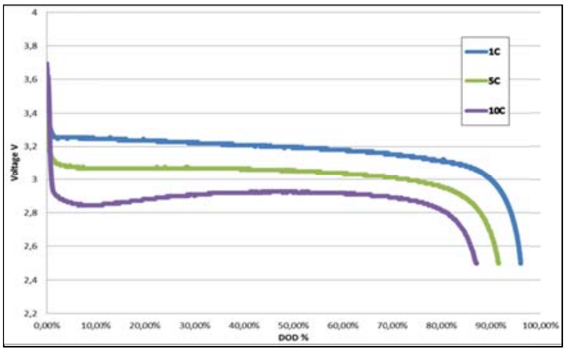


Figure 5 Voltage curves (1C, 5C and 10C) in discharge for soft-pouch cell of 10Ah (type 1; chemistry: $LiFePO_4$)

Figure 6 represents the trend of voltage curves during charge at 1C and 2C for cell type 2 (20 Ah, $LiNiCoMnO_2$).

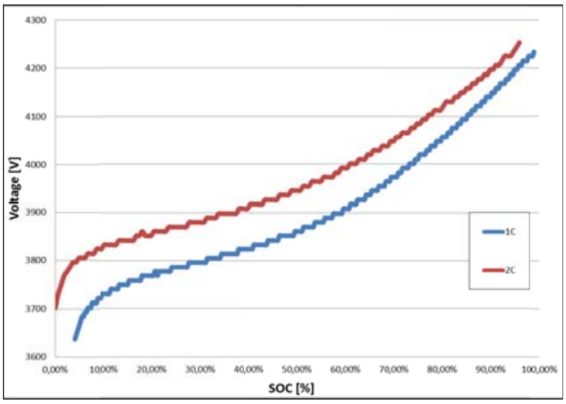


Figure 6 Different profile of charge at 1C, and 2C (soft-pouch cell 20Ah, LiNiCoMnO2)

Figure 7 represents the trend of voltage curves during discharge at 1C, 3C and 10C for cell type 2 (20 Ah, $LiNiCoMnO_2$).
Figure 8 represents the trend of voltage curves during charge at 0.5C and 1C for cell type 3 (150 Ah, $LiFePO_4$).
Figure 9 represents the trend of voltage curves during discharge at 0.3C and 2C for cell type 2 (20 Ah, $LiFePO_4$).
Beside to voltage analysis, the electrical tests allow to monitor the trend of the open-circuit voltage ($E_0$) needed to solve Eq. (6).
Figure 10 shows the trend of OCV (open circuit voltage) for each cell tested. The green line indicates the curve of OCV related to 14 Ah cell ($LiFePO_4$), the red line represents the OCV profile for 20 Ah cell ($LiNiCoMnO_2$), while the blue line is the OCV voltage curve for 150 Ah cell ($LiFePO_4$).
The voltage values are instantly measured at battery terminals during charge or discharge, but the detection of OCV is more complex. During OCV tests, the cells are gradually discharged with step 5% of SOC at constant 0.3C current rate. Between each discharge step there is a cutoff of voltage and a waiting phase to measure the final

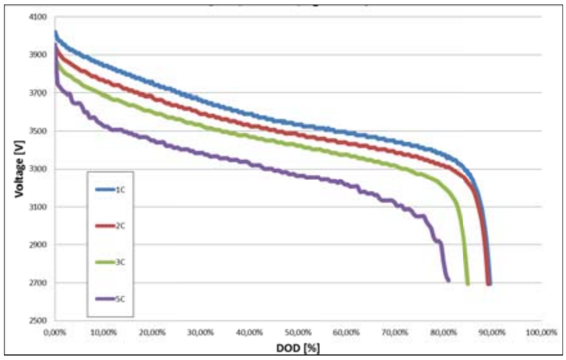


Figure 7 Voltage curves at 1C, 2C, 3C and 5C in discharge for soft-pouch cell of 20Ah (type 2; chemistry: $LiNiCoMnO_2$)

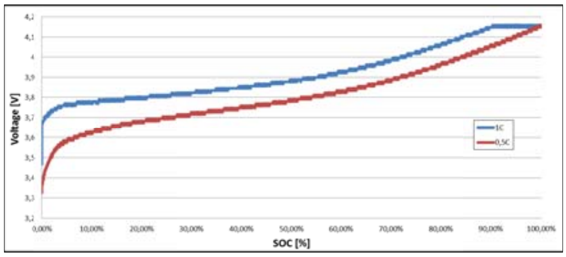


Figure 8 Voltage curves (0.5C and 1C) in charge for soft-pouch cell of 150 Ah (Type 3: chemistry: LiFePO4)

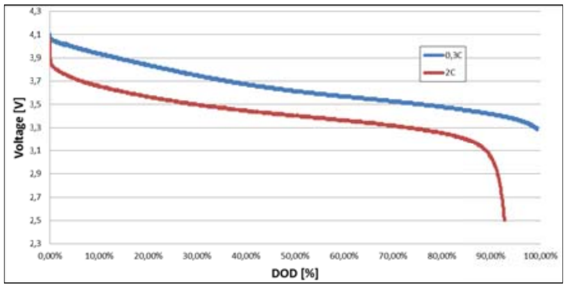


Figure 9 Voltage curves (0.3C and 2C) in discharge for soft-pouch cell of 150 Ah (Type 3: chemistry: $LiFePO_4$)

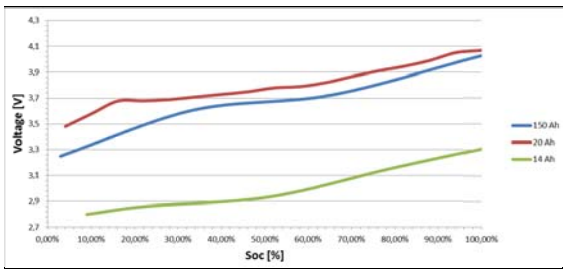


Figure 10 Comparison between OCV curves

OCV value for the related SOC. Usually the waiting phase lasts 8h, but in this case it has been considered 3h of waiting to acquire the OCV values. After a complete discharge, the same cell has been recharged again at 0.3C in 5% step of SOC, in order to obtain two profile of OCV in charge and discharge. Figure 11 shows the report of voltage during the OCV measurements

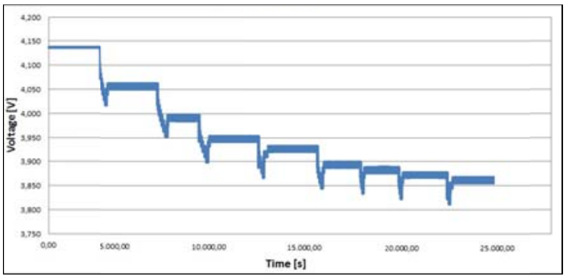


Figure 11 A report of Open Circuit Voltage test for cell type 3 ($LiFePO_4$)

## 4.3 Thermal analysis

In this section the thermal analysis result has been described. The values of heat generated have been calculated solving Eq. (5) and exposed in graphs for each cell.

As cited before, the electrochemical heat source has been evaluated using the parameters previously discussed. The reached temperature has been analyzed by the Eq. (6).

As example, Figure 12 shows the trend of cell heat output valuated by analytical calculation for the 14 Ah cell at 5C current rate. The curve reports the thermal power variation during the discharge cycle. Instead, Figure 13 reports a comparison between the calculation of heat generated at difference current rates: 1C, 5C and 10C.

The thermal condition more severe for cell 14 Ah (type 1 in Table 1) is the discharge at 5C rate, where the output power arrives to 20W.

Table 2 shows the maximum values of thermal power which have been calculated applying the proposed methodology to the selected cells. The reported values concern the sum of contributions due to reversible and irreversible heat generated by electrochemical reactions.

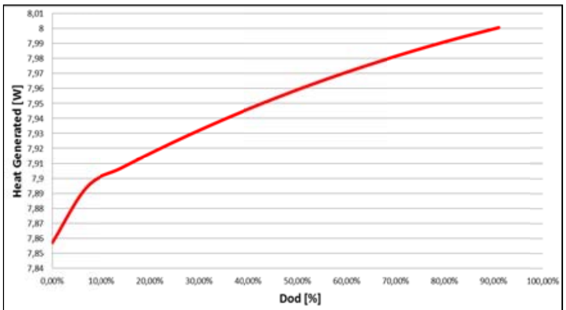


Figure 12 Analytical calculation of heat generated at 5C discharge for 14 Ah cell type 1 ($LiFePO_4$)

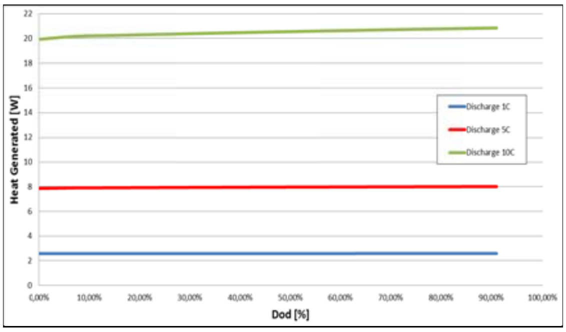


Figure 13 Comparison between the analytical calculation of heat generated at 1C, 5C and 10C discharge for 14 Ah cell type 1 ($LiFePO_4$)

Table 2 Report of thermal power calculated for each cell in charge and discharge mode

| | Type 1 | Type 2 | Type 3 |
|---|---|---|---|
| Charge 1C | 3W | 10 W | 37 W |
| Discharge 1C | 3,5W | 12 W | 42 W |
| Charge 2C | 4W | 23 W | - |
| Discharge 2C | 5W | 27 W | 180 W |
| Discharge 3C | 6,5W | 42 W | - |
| Discharge 5C | 8 W | 170 W | - |
| Discharge 10C | 21 W | - | - |

While the generated heat mostly depends on the operating conditions of the battery, the calculation of battery average temperature is influenced by the environmental external condition, which determinates convective and radiative heat transfer.

In next sections the result regarding the temperature calculation for each selected cell. The trend of temperature is represented in different operating conditions. A comparison between analytical values and real values measured by IR camera is described.

### 4.3.1 Thermal behavior of cell 14 Ah

The cell type 1 with 14 Ah in capacity is the battery with a smaller size than the other analyzed. Despite low capacity, this type of $LiFePO_4$ cell allows to provide high power density. In fact, this cell can be discharged at 10C in continuous. However a current of 140 A (10C mode) in discharge causes a strong increase in temperature, and the designer have to take into account this issue.

Figure 14 shows the trend of temperature in different discharge conditions (1C, 5C and 10C current rate) for the 14 Ah cell. Temperature values have been measured by an IR camera.

Figure 15 and Figure 16 show the difference between the real temperature profile, acquired by an IR camera, and the temperature values calculated by the analytical method. The Figure 15 indicates the trend of temperature measured and calculated for a constant discharge of 10C, while Figure 16 is referred to a constant charge at 1C. In both cases, the gap between the experimental values and those analytical does not exceed 5%.

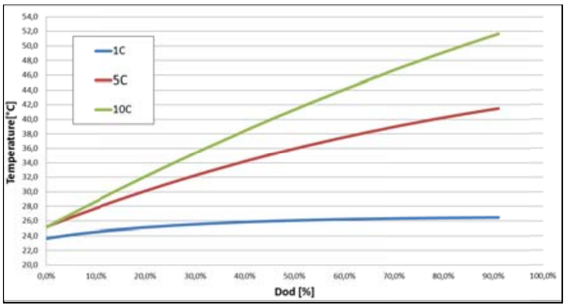


Figure 14 Temperature behavior for different discharge rate (1C, 5C and 10C) of 14 Ah battery.

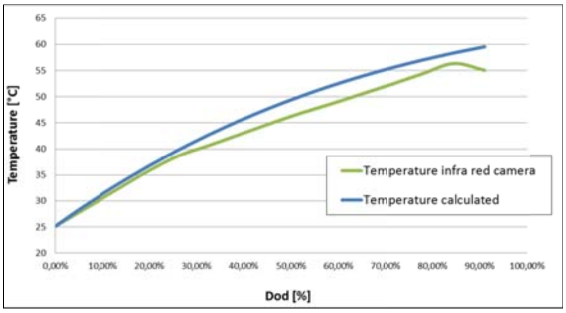


Figure 15 A comparison between the real temperature range for a 10C discharge (acquired by IR camera, green solid line) and the analytical values calculated (blue solid line) for the 14Ah cell model.

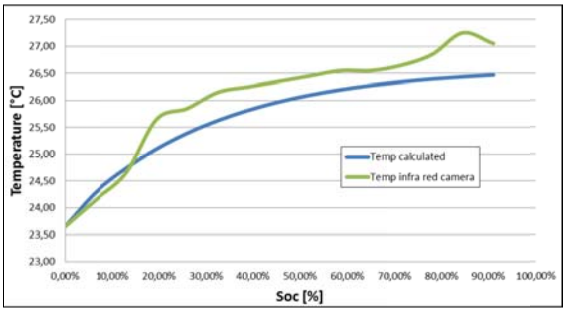


Figure 16 A comparison between the real temperature range for a 1C charge (acquired by IR camera, green solid line) and the analytical values calculated (blue solid line) for the 14Ah cell model

In order to validate the analytical thermal model, in Figure 17 a thermal report regarding the maximum temperature achieved at the end of charge at 1C and discharge at 10C.

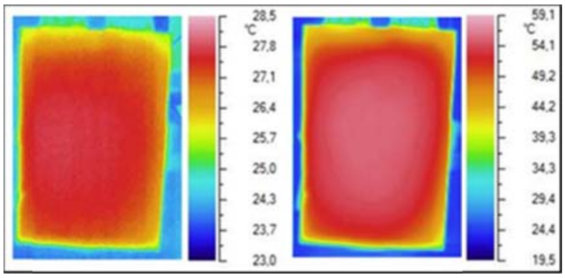


Figure 17 - Thermal images related of charge 1C (on the left) and discharge 10C (on the right)

### 4.3.2 Thermal behavior of cell 20 Ah

The battery with a capacity of 20 Ah is different from the other type for the chemistry of which is constituted. In particular the battery chemistry $LiNiCoMnO_2$ allows to achieve higher voltage peaks than the $LiFePO_4$ cells. However the trends of voltage curves are not constant during charge and discharge phase (Figure 6 - Figure 7). The presence of cobalt makes these battery cells very expensive to produce, but also more profitable to recycle.

Figure 18 shows the trend of temperature in different discharge conditions (1C, 2C and 5C current rate) for the 20Ah cell, where the temperature values have been measured by an IR camera as before mentioned.

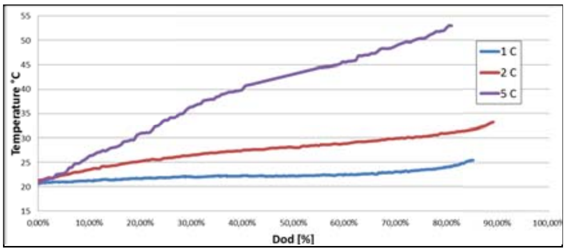


Figure 18 Temperature behavior for different discharge rate (1C, 2C and 5C) of 20 Ah battery

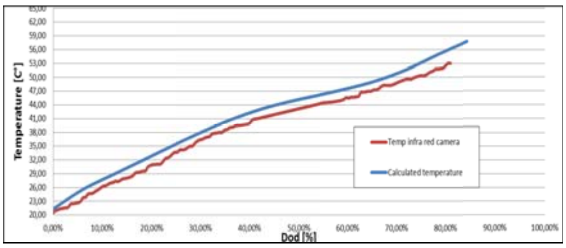


Figure 19 A comparison between the real temperature range for a 5C discharge (acquired by IR camera, green solid line) and the analytical values calculated (blue solid line) for the 20Ah cell model

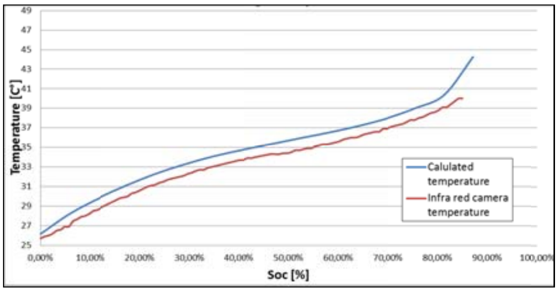


Figure 20 A comparison between the real temperature range for a 3C discharge (acquired by IR camera, green solid line) and the analytical values calculated (blue solid line) for the 20Ah cell model

The Figure 19 reports the comparison between the real temperature profile, acquired by the IR camera, and the temperature values calculated by the analytical method for a 5C discharge. This graphs validate the calculation method for the battery with 20 Ah capacity and chemical type $LiNiCoMnO_2$. Instead Figure 20 shows the comparison between the real temperature profile (IR camera) and the calculated values for a discharge at 3C rate. In both cases it is possible to asses an average error around 5%.

### 4.3.3 Thermal behavior of 150Ah

This type of cell is particularly used in automotive applications due to its high capacity and power density. The chemistry $LiFePO_4$ allows to have an constant voltage during an important part of charge and discharge cycles (Figure 8 - Figure 9).
Figure 21 shows the temperature curves acquired in the tests conducted with a different current rate at 1C (100Ah) and 2C (200Ah) in a continuous discharge phase.

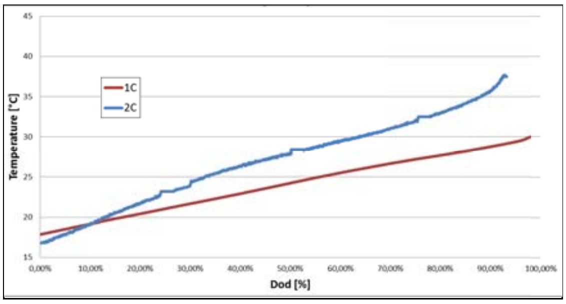


Figure 21 Temperature behavior for different discharge rate (1C and 5C) of 150 Ah battery

The Figure 22 and Figure 23 show the comparison between the analytical temperatures and real values monitored by the IR camera. Particularly, Figure 22 shows the case of a discharge at 300A (3C) where analytical and real values are very close. The Figure 23 shows the differences between the minimum and maximum temperatures monitored by the IR camera (blue and red line) and the curve of analytical temperature calculated (green line) by the described method.

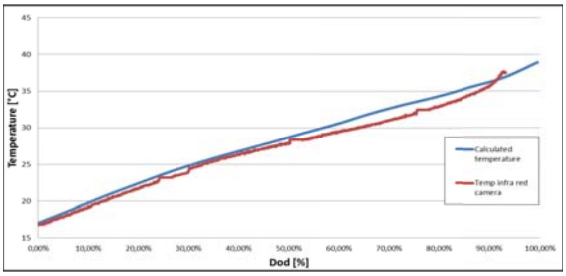


Figure 22 A comparison between the real temperature range for a 2C discharge (acquired by IR camera, green solid line) and the analytical values calculated (blue solid line) for the 150Ah cell model.

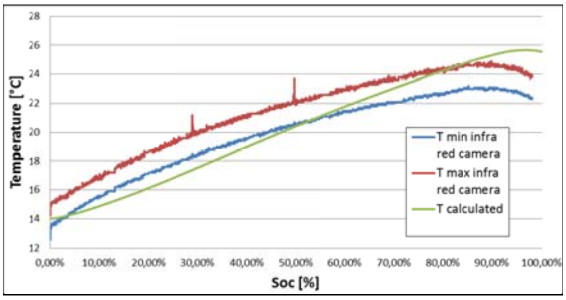


Figure 23 A comparison between the analytical values of temperature (green solid line), calculated for the 150 Ah range for a 1C discharge, and the real temperature profiles acquired by IR camera and related to minus temperature values (blue solid line) and maximum values (red solid line)

## 4.4 Discussion

In the previous sections have been shown the results of analytical calculation applied to continuous charge and discharge at constant current rates. The comparison between calculated temperature values and real behavior shows an average error of almost 5%.

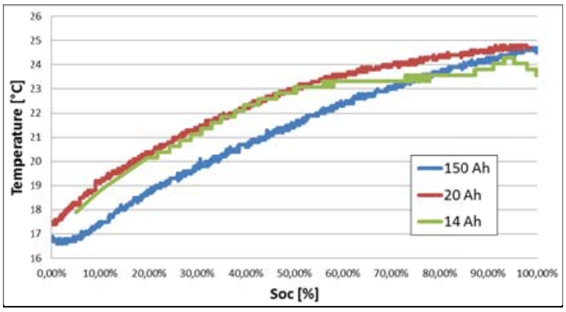


Figure 24 A comparison between the real temperatures reached by each proposed cells during charge at 1C current rate.

The comparison between temperature in charge at continuous 1C rate has been reported in Figure 24 for each analyzed cell of 14 Ah, 20 Ah and 150 Ah. In particular, the blue solid line shows the temperature curve for the cell 150Ah, the red line is related to the cell 20 Ah, and finally the green line regards the cell 14 Ah.

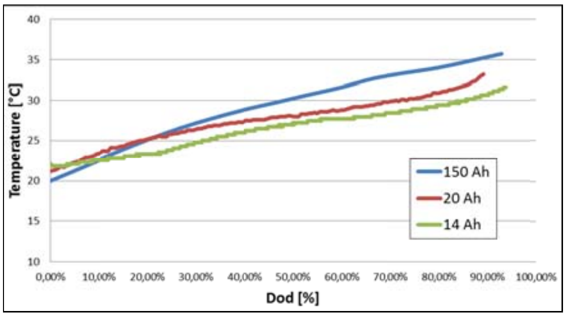


Figure 25 A comparison between the real temperatures reached by each proposed cells during discharge at 2C current rate

Analyzing Figure 24, it is possible to notice that the maximum temperature reached is around 25 °C for each tested cell, although Table 2 reports different levels of heat output calculated for each battery element. The same trend is also shown in Figure 25 where the maximum temperature for discharge at 2C rate is around a range of 31-35°C. These considerations can be explained because the output temperature profile depends not only on the current value and boundary thermal condition, but also on the thermal capacities of each different cell type as reported in the thermal balance in Eq. (6).

# 5 Conclusion

In this paper a methodology has been proposed to guarantee high flexibility, good quality and reduced time to market in the design process of customized battery packs. An electrical and thermal analysis have been applied to calculate the heat generated by the electrochemical reactions of Li-ion battery cells. The proposed approach has been validated for three cases of polymeric Li-ion battery cells that were tested at different current rates of charge and discharge.

The proposed methodology can be extended to the design of a complete battery pack. The calculated values of heat generated, both reversible and irreversible, can be used as input for a FVM analysis. This analysis allows not only to evaluate the maximum temperature achieved during operative condition, but also to simulate the thermal behavior of one Li-ion cell using a 3D virtual model.

Future developments focuses the design of a cell array to study the difference temperature distribution between adjacent battery elements using virtual tool, in order to optimize security and cooling.

# Acknowledgments


The project involves the Università Politecnica delle Marche and FAAM Group, an Italian manufacturer of battery. The authors wish to thank FAAM Group for their precious contribution in the development of this research program.


# References


[1] D. Linden, Handbook of batteries 3rd ed., ISBN 978-0-07-135978-8, New York, McGraw-Hill, 2001

[2] Y. Nishi., Lithium ion secondary batteries; past 10 years and the future, Journal of Power Sources, , 100, pp.101-106, 2001

[3] *D. H.* Jeon et al., Thermal modelling of cylindrical lithium ion battery during discharge cycle, Energy Conversion and Management, 52, pp. 2973-2981, 2011

[4] S. Tobishima, J. Yamaki. A Consideration of Lithium Cell Safety, Journal of Power Sources, volumes 81-82, pp.882-886, 1999

[5] D. Bernardi, E. Pawlikowski, and J. Newman, A General Energy Balance for Battery Systems, Journal of The Electrochemical Society, 132, pp. 5-12, 1985

[6] L. Rao and J. Newman, Heat-Generation Rate and General Energy Balance for Insertion Battery Systems, Journal of The Electrochemical Society, 144, pp. 2697-2704, 1997

[7] K. E. Thomas and J. Newman, Thermal Modeling of Porous Insertion Electrodes, Journal of The Electrochemical Society, 150, pp. A176-A192, 2003

[8] T. M. Bandhauer, S. Garimella, T. F. Fuller, A critical review of thermal issues in lithium-ion batteries, Journal of The Electrochemical Society, 158, 3, R1-R25, 2011

[9] J. S. Hong, H. Maleki, S. A. Hallaj, L. Redey, and J. R. Selman, Electrochemical-Calorimetric Studies of Lithium-Ion Cells, Journal of The Electrochemical Society, 145, pp. 1489-1501, 1998

[10] S. C. Chen et al., Thermal analysis of lithium-ion batteries, Journal of Power Sources, 140, pp.111–124, 2005.

## Authors


Dr. Paolo Cicconi,
PhD. in Mechanical and Management Engineering at PhD School of Università Politecnica delle Marche; doctor thesis: Tools and Methods Based on Knowledge Elicitation to Engineering Design. He graduated in Mechanical Engineering and currently works on research activities regarding Knowledge Management at Industrial Engineering and Mathematical Sciences Department of Polytechnic University of Marche.
Email: p.cicconi@univpm.it

PhD. Student Daniele Landi
Is three years into his PhD studies at the Università Politecnica delle Marche. Currently he is working on methods and tools for virtual prototyping in the Industrial Engineering and Mathematical Sciences Department of the Polytechnic University of the Marche. He graduated in Mechanical Engineering with a thesis entitled: "Study of methods for virtual prototyping".
Email: d.landi@univpm.it

Prof. Michele Germani.
is Associate Professor at the Università Politecnica delle Marche, Department of Industrial Engineering and Mathematical Sciences. His main research topics are: eco-design methods and tools, advanced virtual prototyping tools, energy efficiency and human-machine interaction. He has written 150 scientific papers published in international journals and conference proceedings and he is responsible for several European and National research projects.
Email: m.germani@univpm.it